FERMILAB-CONF-05-166-TD

FIELD QUALITY STUDY IN NB_3SN ACCELERATOR MAGNETS*

V.V. Kashikhin#, G. Ambrosio, N. Andreev, E. Barzi, R. Bossert, J. DiMarco, V.S. Kashikhin, M. Lamm, I. Novitski, P. Schlabach, G. Velev, R. Yamada, A.V. Zlobin, FERMILAB, Batavia, IL 60510, U.S.A.

Abstract

Four nearly identical Nb_3Sn dipole models of the same design were built and tested at Fermilab. It provided a unique opportunity of systematic study the field quality effects in Nb_3Sn accelerator magnets. The results of these studies are reported in the paper.

INTRODUCTION

New generation of superconducting accelerator magnets based on Nb_3Sn superconductor are being developed at Fermilab. These magnets are designed for a nominal field of 10-12 T at 4.5 K temperature. Four shell-type dipole models of HFDA series were built and tested. Magnetic design and parameters of the HFDA models are reported in [1]. The design is based on a two-layer shell-type coil with 43.5 mm bore and a cold iron yoke. Fig. 1 shows cross-sections of the HFDA coil and cold mass.

The coils were wound using keystoned Rutherford-type cable made of 28 Nb_3Sn strands, each 1 mm in diameter. The strands for the first three models HFDA02-04 were produced using the Modified Jelly Roll (MJR) process. The strands for the last HFDA05 model were made using the Powder-in-Tube (PIT) process. MJR strand had higher critical current density J_c and larger effective filament size d_{eff}~100-110 μm whereas PIT strand had lower J_c and smaller d_{eff}~50-60 μm [2]. The cable in HFDA02-03 had 25 μm thick stainless steel core to control the strand crossover contact resistance while the cable of HFDA04-05 was without a core.

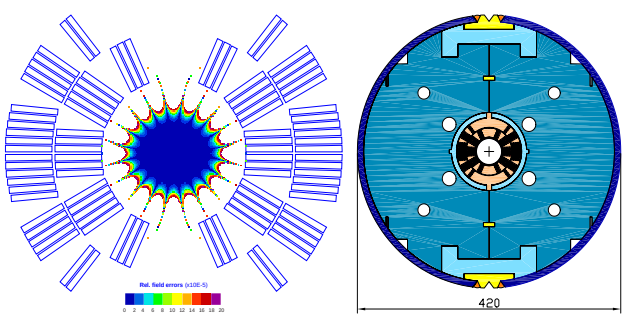

Figure 1: HFDA coil and magnet cross-sections.

QUENCH PERFORMANCE

The models were tested in boiling helium at 4.5 K and lower temperatures. The magnet quench performance is summarized in Fig 2. HFDA02-04 demonstrated similar quench performance with the maximum field of 5-7 T limited by electromagnetic instabilities in MJR strands with large d_{eff} [3]. HFDA05 made of the more stable PIT strand reached its short sample limits of 9.4 T at 4.5 K and 10.1 T at 2.2 K demonstrating reliable performance of the magnet mechanical structure in the above field range [4].

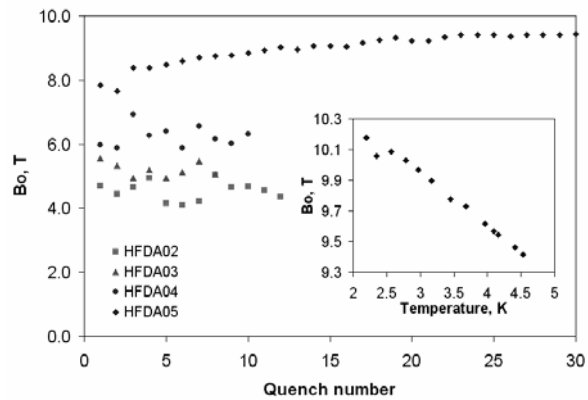

Figure 2: Quench performance of HFDA models.

FIELD QUALITY

Magnetic measurements were performed at 4.5 K using the measurement system described in [5]. The field harmonics are reported at the reference radius of 10 mm using the coordinate system and harmonics definition presented in [5].

Geometrical harmonics

The geometrical harmonics determined as the average values between the current up and down ramps at 3 kA are presented in Table 1.

Table 1: Geometrical field harmonics, 10^{-4}.

n	HFDA02		HFDA03		HFDA04		HFDA05	
	a_n	b_n	a_n	b_n	a_n	b_n	a_n	b_n
2	-9.6	4.1	1.93	-7.13	12.56	0.75	-0.45	4.59
3	-0.2	-4.0	0.81	-2.36	-0.25	8.28	0.90	1.16
4	-1.1	0.4	-0.75	-0.19	0.06	0.16	-1.97	0.79
5	0.3	0.0	0.04	-0.53	0.11	-0.34	0.26	1.94
6	0.3	0.0	0.03	0.12	-0.01	0.02	-0.28	0.22
7	-0.1	0.1	0.03	0.04	-0.03	0.49	0.03	0.29
9	-0.2	-0.2	0.04	-0.01	-0.07	-0.15	-0.01	0.10

HFDA02-03 had large skew or normal quadrupole components. These may occur due to either top-bottom or left-right coil asymmetry created during simultaneous heat treatment of both half-coils assembled without initial prestress.

To check this assumption, the HFDA02 coil with yoke was cut in the straight section and the radial and angular coordinates of each coil block were measured by an optical inspection system. The coordinate system alignment with respect to the coil was established by the midpoints on the pole inserts in the outer layer and the coil-yoke spacers manufactured with a high precision. Fig. 3 shows the coil slice and Table 2 summarizes the

*Work supported by the U.S. Department of Energy
#vadim@fnal.gov

displacements of the six symmetrical block groups from the nominal position and their standard deviations. The block numbering starts from the inner-layer midplane block and ends at the outer-layer pole block as shown in Fig. 3. The positive azimuthal shifts are towards the pole.

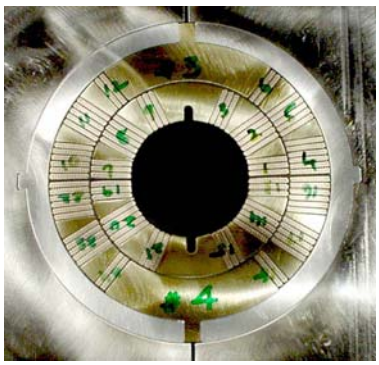

Figure 3: HFDA02 coil cross-section.

Table 2: Deviation of the coil blocks from the nominal position.

Block #	Radial, mm		Azimuthal, mm		Inclination, degrees	
	Δ	σ	Δ	σ	Δ	σ
1	-0.375	0.11	0.102	0.173	0.877	0.476
2	-0.213	0.115	0.161	0.12	1.221	0.391
3	-0.19	0.076	-0.129	0.09	0.941	0.272
4	-0.288	0.09	0.113	0.122	0.444	0.691
5	-0.234	0.062	-0.252	0.129	1.22	0.367
6	-0.094	0.012	-0.285	0.092	0.511	0.22

All coil blocks were systematically shifted towards the aperture center, which is partially related to the coil radial pre-stress from the yoke. One can also see significant deviations of the azimuthal block positions from the design values. These deviations are consistent with the coil geometry re-constructed based on the field quality measurement [5]. For instance, the average measured midplane gap was by ~200 µm larger than the nominal one with ±150 µm standard deviation which is consistent with the predictions [5].

To preserve the nominal coil geometry during fabrication, HFDA04 was heat treated with a thick steel plate introduced between two half-coils. The magnetic measurements showed noticeable improvement of the normal quadrupole component in HFDA04, however, the skew quadrupole associated with the coil top-bottom asymmetry has increased, possibly due to the opposite half-coil orientations with respect to the gravity vector during the coil heat treatment.

The half-coils of HFDA05 were reacted and impregnated separately with the same orientation relatively to the gravity vector. The harmonic measurements in this magnet showed the best geometrical field quality achieved in HFDA models.

Coil magnetization effects

The coil magnetization has persistent current and eddy current components. Both were observed and studied in HFDA models.

The persistent current effect was similar and well predictable in HFDA02-04 made of the same strands. The sextupole hysteretic loops were wide due to high J_c and large d_{eff} in 1-mm Nb_3Sn MJR strands. In order to reduce the persistent current effect, simple passive correctors based on thin iron strips were proposed [6] and successfully tested [7]. Fig. 4 shows the sextupole loops calculated and measured in HFDA03 before and after correction. The passive correction has effectively reduced the sextupole variation in the field range of 1.5-4 T during the field up-ramp from $19.4 \cdot 10^{-4}$ to $3.7 \cdot 10^{-4}$. Excellent correlation of measurements and calculations validated the possibility of prediction and correction of the persistent current effect in Nb_3Sn accelerator magnets.

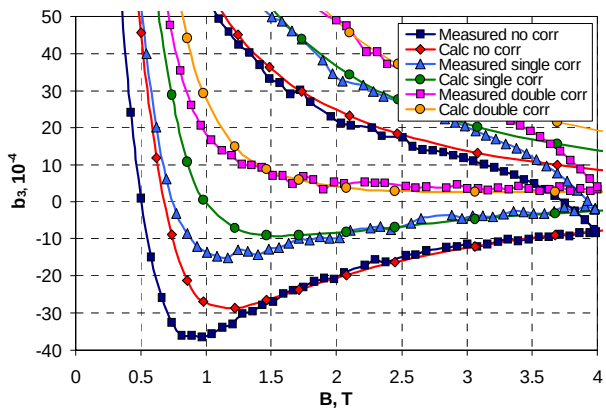

Figure 4: Sextupole hysteresys in HFDA03.

The coil magnetization effect measured in HFDA05 was very different from the other three magnets due to high eddy current component. The values of sextupole component were higher during the up-ramp than during the down-ramp with large ramp-rate dependence as shown in Fig. 5. A similar behavior was observed in SSC dipole DCA312 with a low cable interstrand resistance [8].

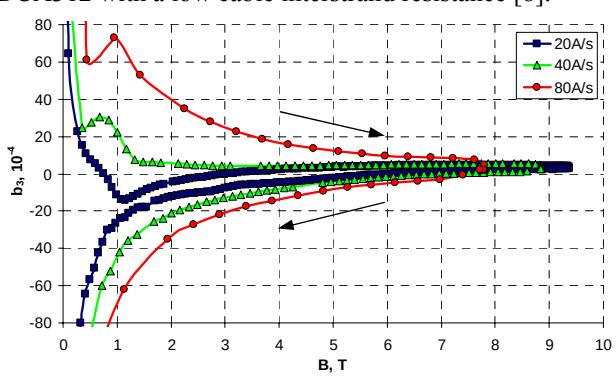

Figure 5: Sextupole hysteresys in HFDA05.

Eddy current effect in sextupole harmonic for HFDA02-05 is shown in Fig. 6, where the sextupole loop width Δb_3, calculated as the difference between field down and up-ramps at Bo=2 T is plotted as a function of the current ramp rate. The models HFDA02-04 show no or very small eddy current effect due to large crossover resistance provided by the stainless steel core inside the cable (HFDA02-03), as well as due to high resistance of

strand matrix (RRR~10) in all the three models. In contrary, the Δb_3 in HFDA05 rapidly changed with the ramp rate and became negative at dI/dt>12 A/s which explains the unusual behavior of HFDA05 harmonics in current cycles. The major difference between HFDA04 and HFDA05 was the high conductivity of the copper matrix in PIT strands after the heat treatment (RRR>50).

The sextupole loop width Δb_3 extrapolated to zero ramp rate is determined by the persistent current component of the coil magnetization proportional to $J_c \cdot d_{eff}$. As it follows from Fig.6, for HFDA05 it is a factor of ~2 lower than for the other three magnets which is consistent with a factor of ~2 smaller effective filament diameter in PIT strand with respect to MJR strand.

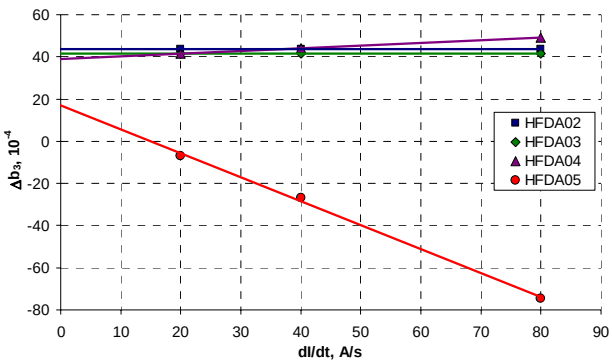

Figure 6: Sextupole loop width at bore field Bo=2 T.

Harmonics decay

The sextupole decays measured at constant currents in HFDA magnets are plotted in Fig. 7. There was no significant b_3 variation during 30 minutes at constant current in HFDA02-04, though a small periodic oscillation in HFDA04 was observed. There was a distinct sextupole variation in HFDA05 that decayed by $8 \cdot 10^{-4}$ during the first 20 minutes at current plateau.

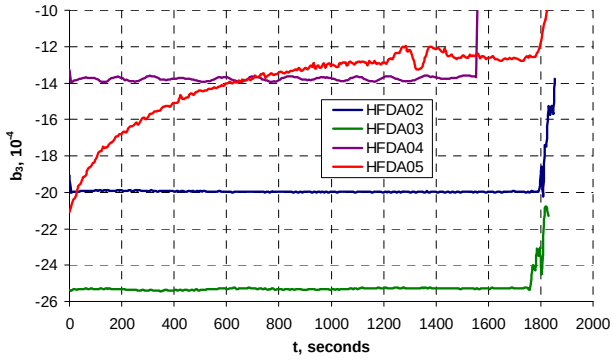

Figure 7: Sextupole decay at I=3 kA (HFDA02-04) and I=2.4 kA (HFDA05).

Iron yoke saturation effect

The HFDA05 magnet reached 10 T field level providing an opportunity to measure the iron saturation effect in HFDA design and compare it with calculations. The measured and calculated reduction of the magnet transfer function in the field range 3-9.4 T were 7.3 % and 8.4 % respectively. Fig. 5 shows that there was no large iron saturation effect in the sextupole up to 10 T that was achieved by special correction holes in iron yoke.

CONCLUSION

Four nearly identical short Nb_3Sn dipole models were fabricated and tested at Fermilab. After improvement of the magnet quench performance in the last model, the nominal design field of 10 T was reached. These models allowed evaluating the field quality in Nb_3Sn accelerator magnets.

The geometrical harmonics were determined by the magnet fabrication tolerances. Significant improvements of low-order geometrical harmonics were achieved after optimizations of the coil fabrication process. There is also room for further improvements.

The coil magnetization effects were determined by the properties of Nb_3Sn strands and cables used in the models. The possibilities of minimizing the persistent current effect by reducing the effective filament size in Nb_3Sn strands and using passive correction techniques were demonstrated. The eddy current effect in all the magnets is well understood. This problem can be alleviated by controlling the interstrand resistance in the Nb_3Sn cables. The difference in harmonic decay observed in the tested magnets needs to be further studied.

The iron saturation effect was suppressed by special holes in the iron yoke in the field range up to 10 T.

REFERENCES

[1] G. Ambrosio et al., "Magnetic Design of the Fermilab 11 T Nb_3Sn Short Dipole Model", IEEE Trans. Appl. Supercond., Vol. 10, No. 1, March 2000, pp.322-325.

[2] E. Barzi et al., "Study of Nb_3Sn Strands for Fermilab's High Field Dipole Models", IEEE Trans. Appl. Supercond., Vol. 11, No. 1, March 2001, pp.3595-3598.

[3] A.V. Zlobin et al., "R&D of Nb_3Sn Accelerator Magnets at Fermilab," 2004 Appl. Supercond. Conf., Jacksonville, FL, September 2004.

[4] A.V. Zlobin et al., "Development and Test of Nb_3Sn Cos-theta Dipoles Based on PIT Strands," Appl. Supercond. Conf., Jacksonville, FL, September 2004.

[5] P. Schlabach et al., "Field Quality of the Fermilab Nb_3Sn High Field Dipole Model", Proc. 2001 Part. Accel. Conf., Chicago, 2001, pp.3418-3420.

[6] V.V. Kashikhin and A.V. Zlobin, "Correction of the Persistent Current Effect in Nb_3Sn Dipole Magnets", IEEE Trans. Appl. Supercond., Vol. 11, No. 1, March 2001, pp.2058-2061.

[7] V.V. Kashikhin et al., "Passive Correction of the Persistent Current Effect in Nb_3Sn Accelerator Magnets", IEEE Trans. Appl. Supercond., Vol. 13, No. 2, June 2003, pp.1270-1273.

[8] A. Ghosh et al., "The Ramp Rate Dependence of the Sextupole Field in Superconducting Dipoles", IEEE Trans. Magn., Vol. 30, No. 4, 1994, pp.1718-1721.